Optica Applicata, Vol. XXV, No. 4, 1995

Thermally induced GRIN effects in cw diode-end pumped lasers

J. K. JABCZYŃSKI, K. KOPCZYŃSKI

Institute of Optoelectronics, Military University of Technology, ul. Kaliskiego 2, 01–489 Warszawa, Poland.

The influence of thermally induced GRIN effects on the output characteristics of cw diode-end pumped lasers was investigated theoretically and experimentally. Several configurations of cavity and pump geometry were examined. The changes of the Rayleigh range, waist size and divergence were observed with the changes of pump power. Satisfactory agreement between theoretical predictions and experimental results was demonstrated. A thermally aberrated Bessel-like beam was observed for high intensities of a pump.

1. Introduction

Despite significantly lower heat load in diode pumped active medium in comparison to lamp pumped one, thermally induced gradients of refractive index (T-GRIN's) play a fundamental role in laser radiation forming in this case [1]–[5]. Depending on the spectrum of diode, active medium properties and cavity parameters, 30%–70% of incident pump power changes into heat [2]. The heat source distribution proportional to pump intensity distribution depends on pumping scheme, diode beam forming optics, absorption properties of active medium and boundary conditions (heat contacts). The gradients of the real part [3], [4] (caused by heat diffusion) as well as the imaginary part [3], [5] (caused by gain distribution) of the refractive index affect output parameters of several diode pumped lasers, from microlasers [4] to high power lasers.

The scope of interest of this paper is focused on low and medium power end pumped solid state lasers. In this case, analytical formulae on temperature distributions are known [6], [7]. The transverse temperature gradients have Gaussian-like shape, whereas longitudinal ones have exponential decay line shape. The thermally induced refractive power of active medium is proportional to the incident pump power in the first order approximation. Thermal lensing determined the Rayleigh range of cavity and the fundamental mode parameters. The ratio of pump caustic size to fundamental mode size has a strong influence on the threshold and efficiency of generation. Further, in the same way, divergence and beam quality depend on these parameters. The second order effects are thermally induced aberrations observed for higher pump intensities [8], [9]. Moreover, in the case of asymmetry of cavity or pump parameters the elliptical beam can be generated [10], [11]. All above effects were observed in our practice of diode pumped lasers and the most interesting effects were examined in detail in the following chapters.

2. Thermal lensing calculations

To calculate refractive power of thermal lensing, temperature distribution in the active medium should be determined. Assuming Gaussian-like heat source distribution, the temperature distribution in active medium can be determined in analytical form [7]. Knowing thermal dispersion dn/dT of active medium, we can calculate the refractive index changes and resulting thermally aberrated wavefront as well as thermal lensing refractive power. In the first order approximation, neglecting non-parabolic components of aberrated wavefront, the refractive power of thermal lens P_T is proportional to pump power P_p as follows:

$$P_T = \beta \cdot P_p \tag{1}$$

where β denotes the thermal sensitivity factor given by

$$\beta = \frac{1}{kA_p} \frac{dn}{dT} f(D_c, l_c, A_p, \ldots) \tag{2}$$

where k denotes the thermal conductivity of the active medium, A_p denotes the averaged pump area, $f(D_c, l_c, A_p, \ldots)$ denotes complicated function of a diameter D_c and length l_c of the active medium, pump shape and size, *etc.* Let us consider thermo-optical parameters of three typical laser crystals (Tab. 1).

Table 1. Thermo-optical parameters of three laser crystals

	Nd:YAG	Nd:YVO_4	Nd:YLF
Thermal conductivity k [W/m/K]	13	5.23 $\parallel c$ 5.10 $\perp c$	7.2 $\parallel c$ 5.8 $\perp c$
Thermal expansion coefficient α [10^{-6}/K]	6.96	11.37 $\parallel c$ 4.43 $\perp c$	8 $\parallel c$ 13 $\perp c$
Thermal dispersion dn/dT [10^{-6}/K]	7.3	3.0 $\parallel c$ 8.5 $\parallel c$	−4.3 $\parallel c$ −2.0 $\perp c$
Refractive index n for $\lambda = 1.06$ μm	1.82	2.16 $\parallel c$ 1.95 $\perp c$	1.47 $\parallel c$ 1.45 $\perp c$

From the thermal lensing viewpoint the worst of the above three is Nd:YVO_4. However, this crystal has other properties advantageous in the case of low and medium power or pulse Q-switched applications. We intended to compare Nd:YVO_4 laser thermal lensing properties to those of the Nd:YAG laser for several cavity parameters.

We calculated the temperature distributions for three types of lasers (two for Nd:YAG, one for Nd:YVO_4), which were examined in experiments (see Figs. 1**a** and **b**). The resulting temperature increase for three pump levels, assuming the circular pump size with diameter of 250 μm, is presented in Tab. 2.

In all three cases, the crystal length was sufficient to absorb more than 95% of incident pump power. It was found that the ratio of crystal to pump diameter

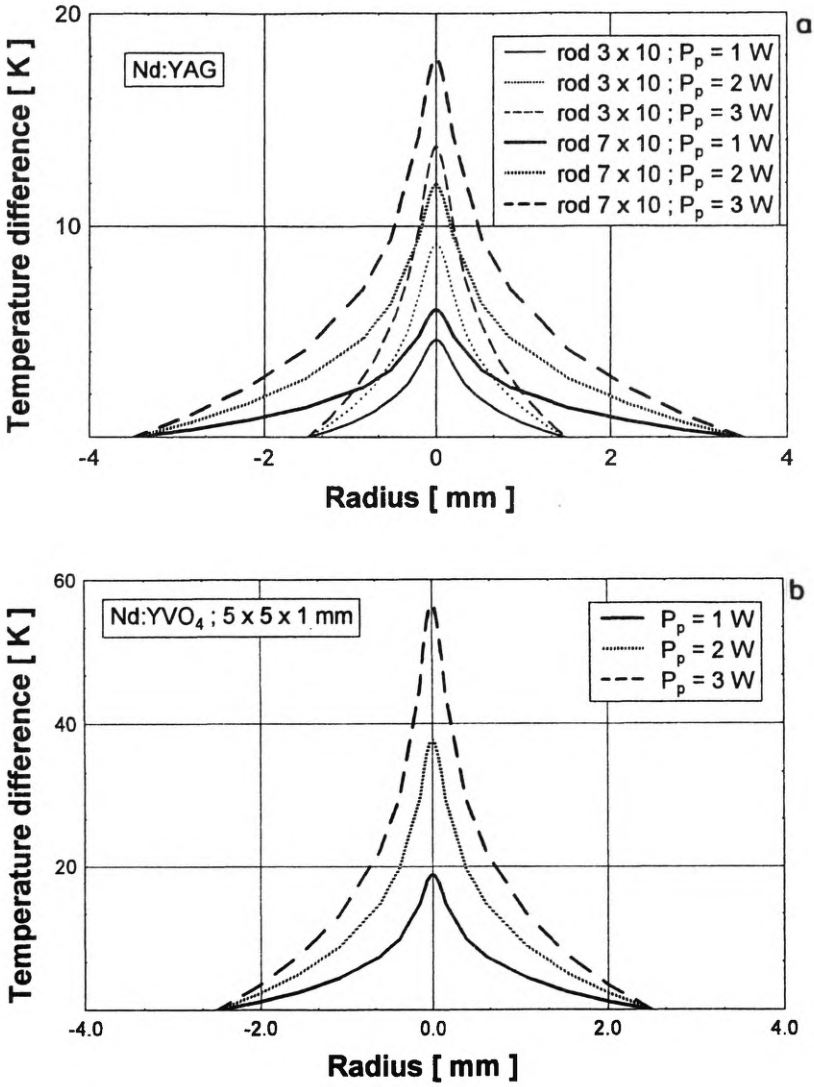

Fig. 1. Temperature distributions in the rear facet of active medium for two Nd:YAG (a) and for Nd:YVO_4 (b) crystals and three pump powers

Table 2. Temperature increase for three values of pump power and crystals with different parameters

	ΔT [K]		
Pump power	Nd:YAG, $\Phi = 3$ mm	Nd:YAG, $\Phi = 7$ mm	Nd:YVO_4, $\Phi = 5$ mm
1 W	4.56	5.96	18.81
2 W	9.13	11.92	37.63
3 W	13.69	17.88	56.44

does not considerably affect the temperature difference in our cases. The significantly stronger influence of thermal conductivity results in about three times stronger thermal sensitivity of Nd:YVO_4 in comparison to Nd:YAG. Thus, we decided to measure the thermal refractive power for these two crystals in order to experimentally determine the thermal sensitivity factor and compare it with the theory.

3. Thermal lensing measurements

To determine thermal lensing we measured the parameters of output beam (see, *e.g.*, [12]) generated in a cavity consisting of the given active medium with a mirror deposited on it and a flat output coupler located at a distance of 110 mm from the rear mirror of the cavity (see Fig. 2).

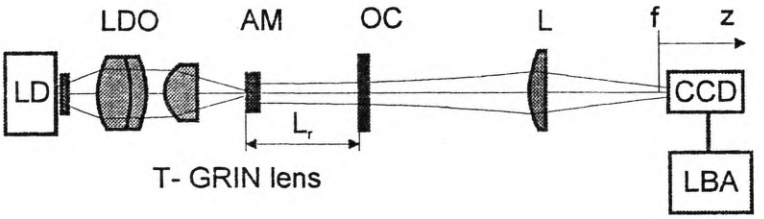

Fig. 2. Scheme of the experimental set: LD – laser diode LDT270004, LDO – laser diode optics, AM – active medium which is T-GRIN lens, OC – output coupler, L – lens, CCD – CCD camera, LBA – laser beam analyser

In the case of a flat-flat cavity with a lens of refractive power P_T located on the rear mirror, the *ABCD* round trip matrix is given by

$$\begin{bmatrix} A & B \\ C & D \end{bmatrix} = \begin{bmatrix} 1-2P_T & 2L_r(1-L_rP_r) \\ -2P_T & 1-2P_T \end{bmatrix}. \tag{3}$$

Applying the formula of the Rayleigh range Z_R for the given *ABCD* matrix of a resonator (see, *e.g.*, [13]) after a few manipulations we obtain

$$Z_R = \sqrt{L_r(1/P_T - L_r)}. \tag{4}$$

Let us notice that the upper stability limit of a resonator is determined by a thermal lens of the focal length P_T^{-1} equal to the cavity length L_R. To determine P_T one should know the Rayleigh range of a laser and its cavity length. From Eq. (4) we derived the following formula on the thermal refractive power:

$$P_T = \frac{L_r}{Z_R^2 + L_r^2}. \tag{5}$$

Formulae (4) and (5) were used to compare the results of experiments with theoretical calculations based on formulae (1) and (2). The Rayleigh range was calculated from the data of beam diameter measurements carried out in several sections in the vicinity of the focal plane of the lens L (see Fig. 2). After calculating

waist locations, diameter, and caustic length in the image space of lens the same parameters were determined in the object space using formulae on propagation of multimode beam in paraxial systems (see *e.g.*, [14]). We carried out measurements of the Rayleigh range in dependence on the pump power (0.9 – 1.8 W) for three cases described in Chapt. 2. As a rule, near diffraction limited, circular beam (with ellipticity < 1.05) was obtained in majority of experiments for low and medium pump levels. Applying a knife edge criterion with clip level 0.1 of beam diameter definition, the dependence of beam diameter on pump power and distance to the lens was investigated. As can be seen in Fig. 3, the image waist is shifted to the focal point of a lens and the resulting Rayleigh range decreases with pump power increase.

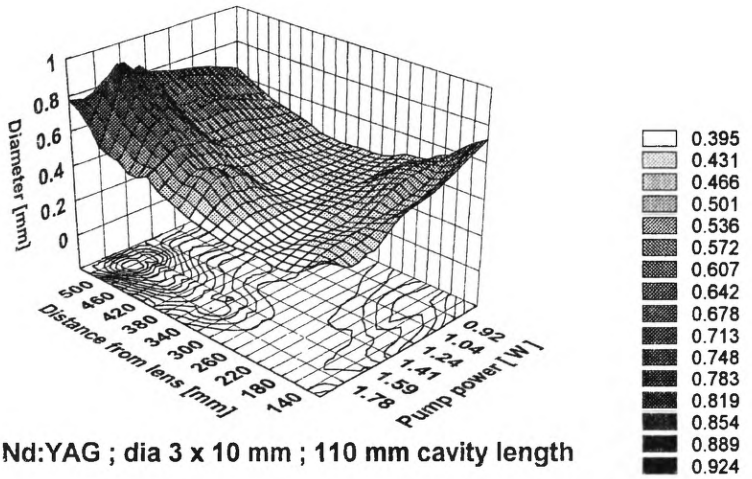

Fig. 3. Beam diameter after passing through a lens *vs.* the distance from the lens and pump power

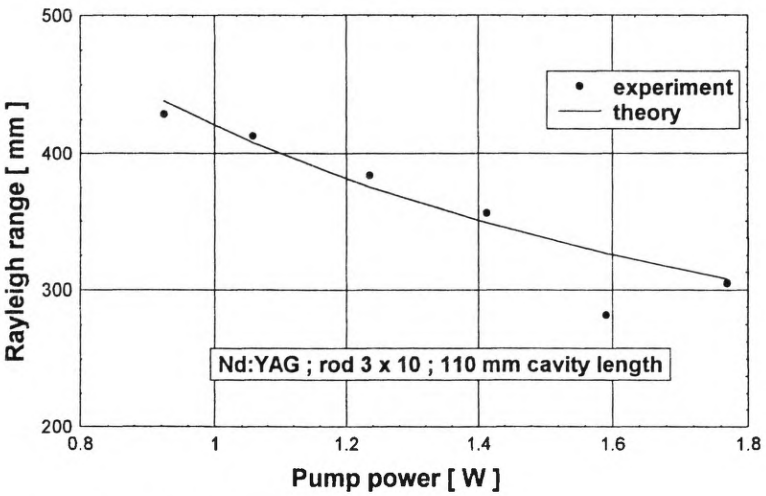

Fig. 4. The Rayleigh range *vs.* pump power

Let us consider (Fig. 4) typical dependence of the Rayleigh range on pump power. As a rule, Rayleigh range decreases with pump power [4]. The results of refractive power measurements are presented in Fig. 5.

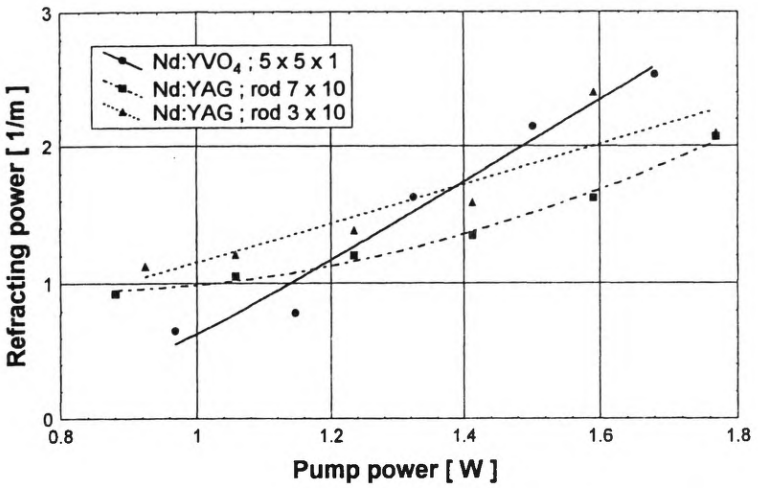

Fig. 5. Thermal refractive power *vs.* pump power for three cases

The relation between pump power and thermal refractive power was approximately linear. Through applying linear regression we determined experimental values of the thermal sensitivity factor β as the slope of the linear regression line. As presented in Tab. 3, the thermal sensitivity of Nd:YVO_4 is significantly higher than that of Nd:YAG.

Table 3. Results of thermal sensitivity calculations and measurements

	β [W^{-1} m^{-1}]		
	Nd:YAG $\Phi = 3$ mm	Nd:YAG $\Phi = 7$ mm	Nd:YVO_4 $\Phi = 5$ mm
Experiment	1.17	1.38	2.88
Theory	1.32	1.45	3.4

The satisfactory agreement between theory and experiment was achieved for all three cases. However, as it will be presented in the next chapter, the thermal lensing limited to an aberration free effect is not a satisfactory explanation of phenomena observed for high pump densities. Also for low value of power slightly above the threshold one, the laser beam is determined rather by gain guiding because the thermal lensing is very weak and the fundamental mode volume of flat-flat cavity is large compared to the pump volume.

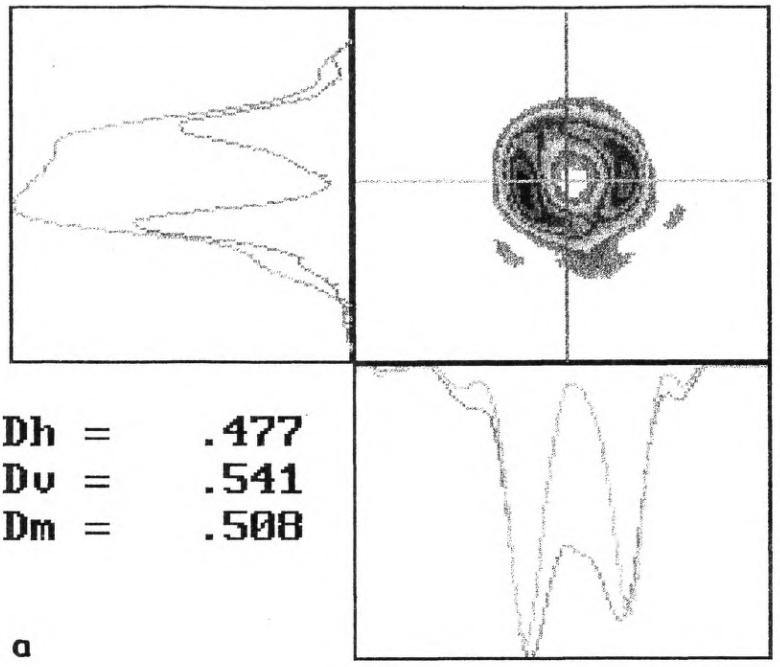

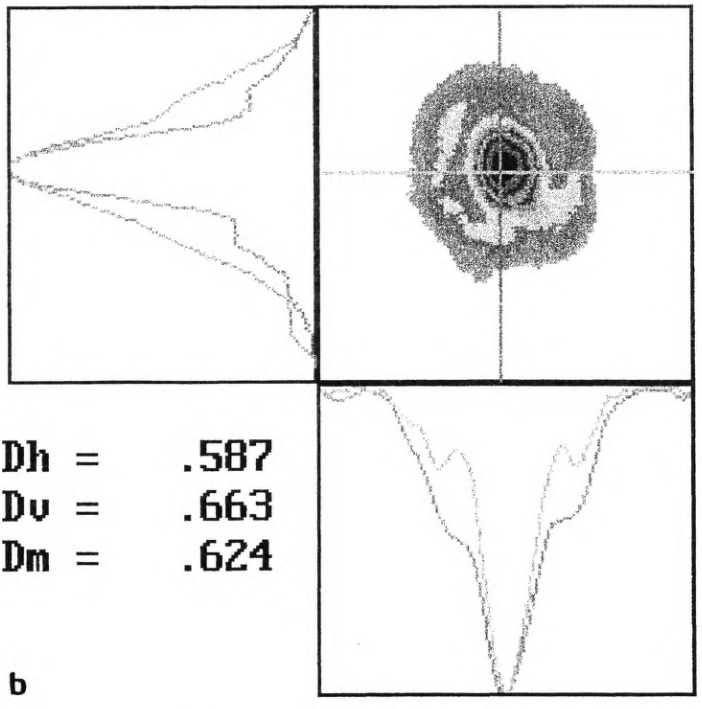

Fig. 6. Intensity distributions in the plane 320 mm distant from the lens, Nd:YVO_4 crystal, 1.6 W pump power (a), in the plane 360 mm distant from the lens, Nd:YVO_4 crystal, 1.6 W pump power (b)

4. Thermally aberrated beam

For the higher pump densities the temperature distributions cause the non-parabolic distortion of a beam wavefront. It was observed for Nd:YAG crystal as well as for Nd:YVO_4 crystal that outside the caustic region the intensity distributions have atypical shapes. In one plane (Fig. 6a) the annular intensity was registered, whereas a few centimetres away from it the Bessel-like shape was observed (Fig. 6b).

The non-monotonic distribution along the optical axis with maxima and minima of intensity was observed (Figs. 7a, 7b). Such unusual intensity distribution suggests that the conical as well as spherical aberration [8], [9] components should exist in the aberrated wavefront.

It is difficult to determine the beam quality parameter of such a beam because of the non-Gaussian shape of intensity distribution. The traditional criteria of beam definition (FWHM, $1/e^2$) cannot be used for such atypical beam. For beam diameter defined from knife edge criterion, slightly oscillated dependence of diameter on length along optical axis was observed (Fig. 8).

However, the caustic length defined as a distance from the waist, where the beam area increases twice, is much longer compared to Gaussian beam observed for low pump power. This property is similar to the Bessel beam behaviour. However, the influence of the higher order aberrations causes the occurrence of much more complicated ring intensity distributions.

Similar ring distributions were observed by FRAUCHINGER *et al.* [3] for near semi-concentric resonator, however, they did not observe the non-Gaussian distributions for flat-flat cavity. A different explanation of the non-Gaussian intensity distribution has been proposed by LONGHI and LAPORTA [15] lately. They

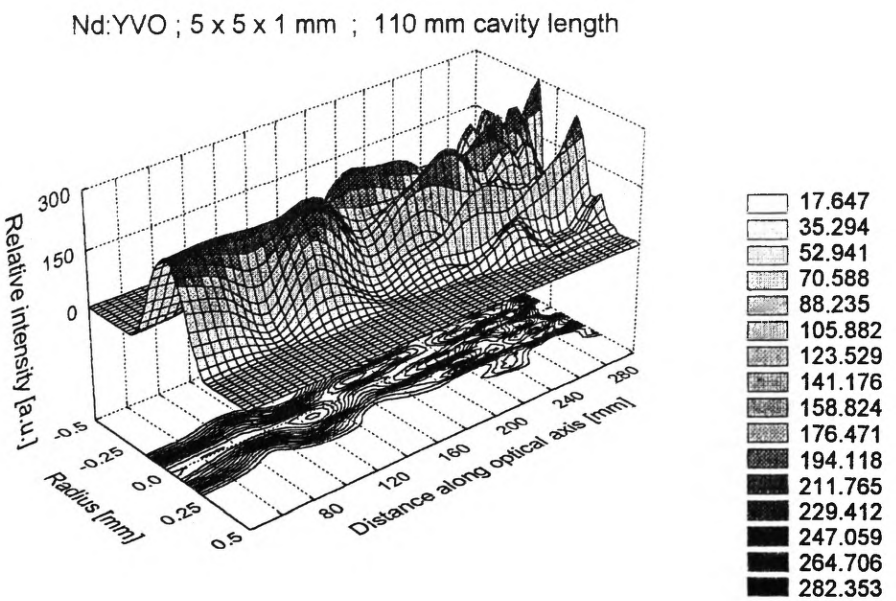

Fig. 7a

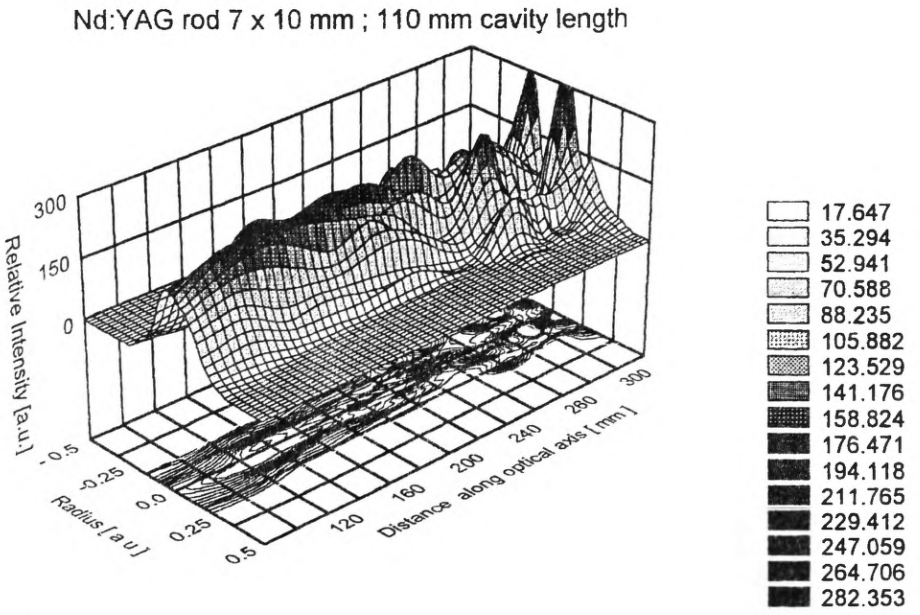

Fig. 7b

Fig. 7. 3-D plot of intensity distribution of thermally aberrated beam: Nd:YVO_4 laser, pump power 1.8 W (a); Nd:YAG laser, pump power 1.8 W (b)

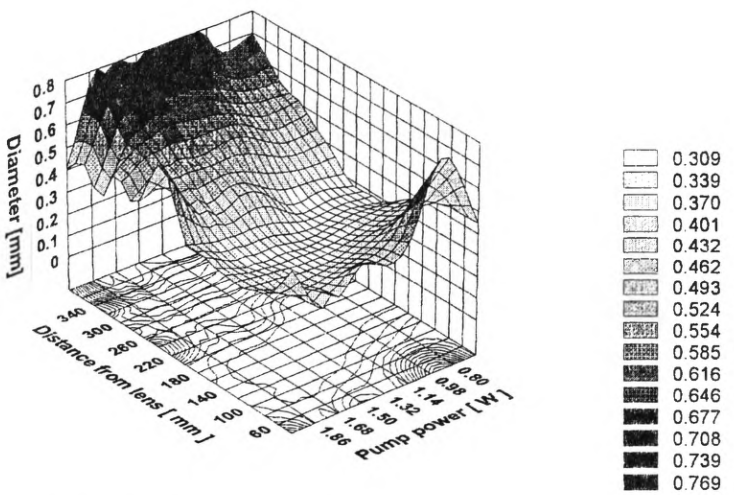

Nd:YVO_4 ; 5 x 5 x 1 mm ; 110 mm cavity length

Fig. 8. Beam diameter after passing through the lens *vs.* the distance from the lens and pump power

found that in a cavity with a high gain, the conical emission with either annular or Bessel shape is possible.

In our case, the fundamental mode diameter calculated from thermal lensing data was larger than the pump size. There was generated the fundamental mode with aberrated wavefront, in contrast to the results reported in [3], where the higher order modes were excited. We conclude that due to high gain and refractive index gradients, we observed the special form of fundamental mode distribution, called the aberrated Gaussian beam. We suppose that it is, to our knowledge, the first experimental demonstration of such an effect, and it will be the subject of further investigations.

5. Conclusions

It was shown experimentally that performance of the cw diode-end pumped solid state lasers is determined by an induced T-GRIN effect. As a rule, the thermal lensing refractive power increases and the waist diameter decreases with pump power, but its magnitudes also significantly depend on thermal contacts of active medium, pump beam sizes and cavity parameters. The refractive power of T-GRIN was determined from measurements of the Rayleigh range of the output beam. The experimental results were compared with theoretical ones based on paraxial matrix approach and assumed radial temperature gradients in the rod. The satisfactory agreement between the theory and experiment was achieved. Near diffraction limited, circular beam was obtained in majority of experiments for low and medium pump power. For higher pump levels, thermally aberrated beam was observed with the annular Bessel shape. The beam quality definition could not be applied for such non-Gaussian beam.

Acknowledgements — We would like to thank Prof. Maksymilian Pluta for inspiration of active GRIN research. This work was supported by the Polish Committee for Scientific Research (KBN) under the grant T11B00708. All coatings were made by Dr M. Trnka from COBRABiD, Warsaw, Poland.

References

[1] FAN T. Y., BYER R. L., IEEE J. Quantum Electron. **24** (1988), 895.
[2] CHEN T. S., ANDERSON V. L., KAHAN O., IEEE J. Quantum Electron. **26** (1990), 6.
[3] FRAUCHINGER J., ALBERS P., WEBER H. P., IEEE J. Quantum Electron. **28** (1992), 1046.
[4] ZAYHOWSKI J. J., *OSA Proc. Advanced Solid State Lasers '90*, 1990, Vol. 6, p. 9.
[5] SALIN F., SQUIER J., Opt. Lett. **17** (1992), 1352.
[6] KOECHNER W., *Solid-State Laser Engineering*, Springer-Verlag, Berlin, Heidelberg, New York 1988.
[7] COUSINS A. K., IEEE J. Quantum Electron. **28** (1992), 1057.
[8] HODGSON N., WEBER H., IEEE J. Quantum Electron. **29** (1993), 2497.
[9] BECKMAN L., *Proceedings of Optical Design Conference*, Rochester 1994.
[10] CZARSKE J., MULLER H., Opt. Commun. **114** (1995), 223.
[11] TACCHEO S., LAPORTA P., LONGHI S., SVELTO C., Opt. Lett. **20** (1995), 889.
[12] NEUNSCHWANDER B., WEBER R., WEBER H. P., IEEE J. Quantum Electron. **31** (1995), 1082.
[13] BURCH G., *Introduction to Matrix Method in Optics*, J. Wiley, London 1975.
[14] SIMON R., MAKUNDA N., SUDARSHAN E. C. G., Opt. Commun. **65** (1988), 322.
[15] LONGHI S., LAPORTA P., J. Opt. Soc. Am. B **12** (1995), 1511.

Received November 6, 1995